Journal of
Nanoscience and Nanotechnology
Vol. 10, 7808–7811, 2010

Subsurface Damage of Single Crystalline Silicon Carbide in Nanoindentation Tests

Jiwang Yan[1,*], Xiaohui Gai[2], and Hirofumi Harada[3]

[1] *Department of Nanomechanics, Tohoku University, Aramaki Aoba 6-6-01, Aoba-ku, Sendai 980-8579, Japan*
[2] *Department of Metallurgy, Material Science and Material Processing, Tohoku University, Aramaki Aoba 6-6-02, Aoba-ku, Sendai 980-8579, Japan*
[3] *Siltronic Japan Corporation, 3434 Shimata, Hikari, Yamaguchi 743-0063, Japan*

The response of single crystalline silicon carbide (SiC) to a Berkovich nanoindenter was investigated by examining the indents using a transmission electron microscope and the selected area electron diffraction technique. It was found that the depth of indentation-induced subsurface damage was far larger than the indentation depth, and the damaging mechanism of SiC was distinctly different from that of single crystalline silicon. For silicon, a broad amorphous region is formed underneath the indenter after unloading; for SiC, however, no amorphous phase was detected. Instead, a polycrystalline structure with a grain size of ten nanometer level was identified directly under the indenter tip. Micro cracks, basal plane dislocations and possible cross slips were also found around the indent. These finding provide useful information for ultraprecision manufacturing of SiC wafers.

Keywords: Nanoindentation, Silicon Carbide, SiC, Subsurface Damage, Phase Transition, Semiconductor Manufacturing.

1. INTRODUCTION

Single crystalline silicon carbide (SiC) is a next-generation semiconductor material for advanced power devices and micro/nano electromechanical systems (MNEMS). Compared with silicon, SiC has much higher thermal conductivity, higher current density, higher breakdown electric field strength and broader band gap; thus, it is an excellent material for high-temperature, high-frequency and high-power applications.[1] The manufacturing of damage-free precision SiC wafers is an essential technical step for device manufacturing. However, due to its high hardness and high brittleness, SiC is very difficult to machine. Thus, the difficulty in wafer manufacturing is one of the main problems limiting the development of SiC device technology.

To improve wafer integrity, subsurface damage generated by micro/nano machining is an emerging research focus from multidiscipline researchers.[2] Since the mechanical contact in an indentation test is geometrically akin to that in a machining process, understanding the indentation-induced material deformation, microfracture and microstructural change can provide useful information for wafer manufacturing to eliminate machining damages.[3,4] However, to date, literature on indentation-induced damage of single crystalline SiC is still very limited.[5–7] A few fundamental aspects, such as, the subsurface damage mechanism, the relationship between the damage depth and the indentation depth, have not been clarified. Whether crystalline SiC undergoes amorphization in nanoindentation tests or not is still a controversial issue.

In the present paper, we investigated the responses of single crystalline SiC to a sharp Berkovich nanoindenter at various loads. The indentation-induced damage was investigated by examining the load-displacement curves and the residual indents using transmission electron microscope (TEM) and the selected area electron diffraction (SAED) techniques.

2. EXPERIMENTAL DETAILS

A nanoindentation tester, ENT-1100a, produced by Elionix Co. Ltd., was used for the experiments. Tests were performed using a Berkovich indenter made of single crystalline diamond. This kind of indenter is geometrically akin to an extremely sharpened single point diamond tool in an ultraprecision machining process. The maximum load was varied from 10 mN to 100 mN by an increment of 10 mN, and then changed from 100 mN to 1000 mN by an increment of 100 mN. The time for

*Author to whom correspondence should be addressed.

 1533-4880/2010/10/7808/004 doi:10.1166/jnn.2010.2895

loading and unloading was the same and fixed to 5 s; thus, the loading/unloading rate changed in the range of 0.2∼40 mN/s. The holding time was 1 s. Ten indentation tests were made for each maximum load, and the pitch between every two neighboring indents was set to 25 μm.

A nitrogen-doped N-type single-crystal 6H–SiC wafer with a surface orientation of (0001) silicon face was used as the specimen. It has a hexagonal structure (zinc-blende structure) and the lattice parameters are $a = 3.081$ Å and $c = 15.117$ Å. The wafer was 50.8 mm in diameter, 0.234 mm in thickness and obtained with a chemomechanical polished finish. The SiC wafer has a Mohs hardness of ∼9. The circumferential orientation of the SiC wafer to the indenter was adjusted to make the orientation flat $[10\bar{1}0]$ parallel to one face of the indenter. Thin-foil specimens for cross-sectional TEM (XTEM) observation were prepared using a focused ion beam (FIB) apparatus in such a way that the specimen contains the loading direction and the center of the indent. These specimens were then examined using a TEM, Hitachi H-9000NAR, at an accelerating voltage of 300 kV. Selected area electron diffraction (SAED) was performed using the same TEM at a camera length of 1.0 m and a field area having a diameter of 100 nm.

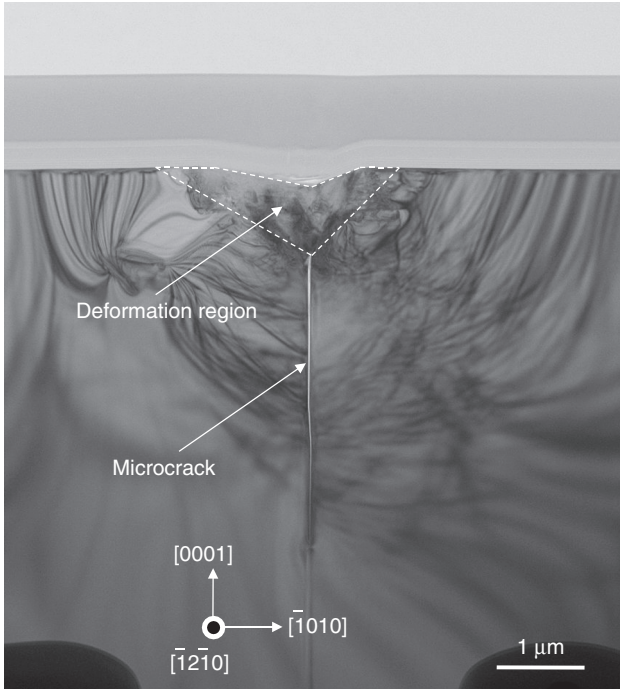

Fig. 1. XTEM micrograph of an indent generated at a maximum load of 100 mN, showing a region of subsurface deformation and a microcrack extending into the bulk.

3. RESULTS AND DISCUSSION

3.1. XTEM Observation

Figure 1 is a bright field XTEM micrograph of an indent made at a maximum load of 100 mN. The long stripes seen cross the entire field are interference fringes caused by the bending of the TEM sample due to FIB processing. It is seen that just below the indent surface, there is a region of intensive material deformation as indicated by the dotted line, the depth of which is approximately 1 μm. The depth of material deformation is 2.5 times that of the maximum indentation depth (0.4 μm) and 5 times that of the residual depth of the indent (0.2 μm) identified from the corresponding load-displacement curves. Below the deformation region, a long microcrack (median crack) extends straightly downwards to a depth of approximately 4 μm. This result indicates that the critical condition for crack initiation has been exceeded at this load, although there were no cracks observed on the wafer surface under this condition. That is to say, subsurface cracks take place at a smaller load than surface cracks. The relationship between damage depth and indentation depth in this study is similar to that of 4H–SiC in previous works.[5, 6] However, for 4H–SiC, the first cracks to form were lateral and radial microcracks,[5] rather than median cracks. This difference in cracking behavior might be a result of difference of crystalline structure between 4H– and 6H–SiC.

Figures 2(a) and (b) are magnified views of the left side and the right side of the indent shown in Figure 1. The regions indicated by circles A and B in Figure 2(a) are for SAED analysis. Different from that of silicon indentation[8] where beneath the indent a low-contrast grey region was generated due to the amorphization of silicon; in Figure 2, however, the deformation region shows a non-uniform contrast, indicating that the strain is significant and strain distribution is not uniform. In silicon indentation,[8] distinct boundaries between the amorphous region and the surrounding region could be identified; in Figure 2, however, the boundaries between the deformation region and the surrounding region are not very clear. In Figure 2(b), dislocations on the basal plane (0001) can be clearly identified on the right side of the indent. A dislocated region (the dark area indicated by the arrow) is expanding downward from the basal plane, indicating that cross slipping with other planes, such as the pyramidal plane $\{10\bar{1}3\}$ and the prismatic plane $\{10\bar{1}0\}$, might have occurred, although the Burgers vector of these dislocations cannot be clearly indentified under the present conditions.

It is known that the slip systems of single crystalline SiC are $(0001)\langle 1\bar{2}10\rangle$, $(0001)\langle 01\bar{1}0\rangle$, $\{10\bar{1}3\}\langle 1\bar{2}10\rangle$ and $\{10\bar{1}0\}\langle 1\bar{2}10\rangle$. Under a load in [0001] direction, the Schmid factors for these slip systems are 0.378, 0.282, 0.131 and 0.019, respectively.[9] Dislocations of SiC are most likely to take place on the basal plane slip along $(0001)\langle 1\bar{2}10\rangle$ or $(0001)\langle 01\bar{1}0\rangle$; cross slips along

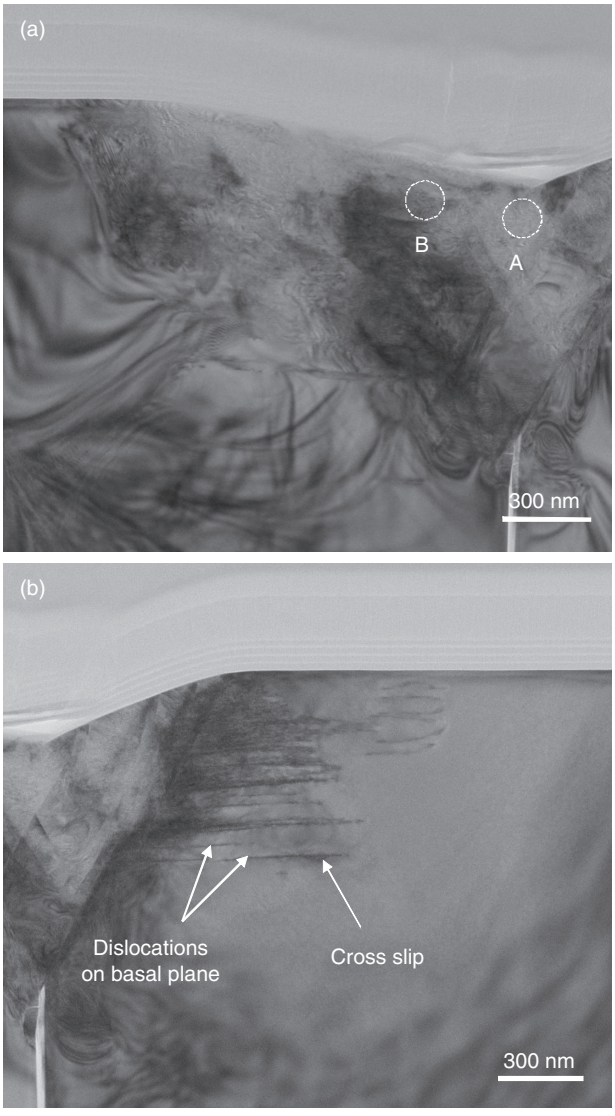

Fig. 2. Magnified views of (a) left side and (b) right side of the same indent as that in Figure 1. Circles A and B in (a) indicate regions for SAED analysis; in (b), basal plane dislocations and cross slip can be identified.

$\{10\bar{1}3\}\langle 1\bar{2}10\rangle$ and $\{10\bar{1}0\}\langle 1\bar{2}10\rangle$ may also take place if specific conditions are satisfied.

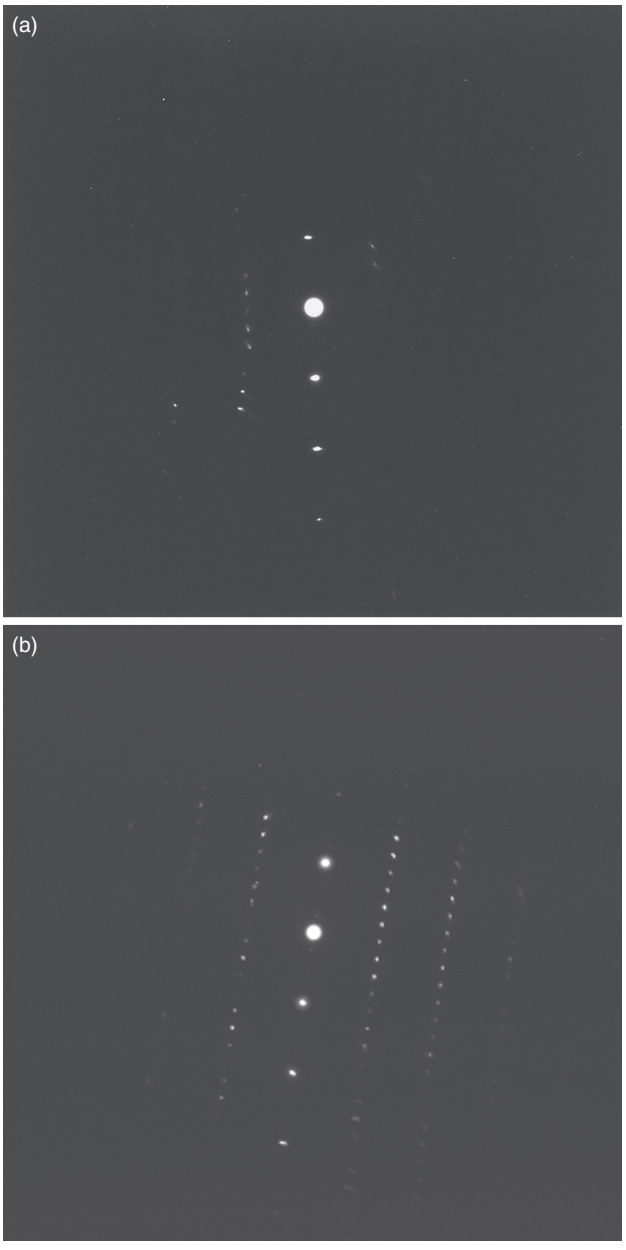

Fig. 3. SAED patterns of the selected regions (a) A and (b) B indicated in Figure 2(a), showing a poly crystalline structure and a strained single crystalline structure, respectively.

3.2. SAED Analysis

Figures 3(a) and (b) are SAED patterns of the regions A and B indicated in Figure 2(a). In both figures, only diffraction spots of $[10\bar{1}0]$ incidence can be seen and no halo rings can be identified. Therefore, we can say that SiC did not undergo amorphization under the present indentation conditions. In Figure 3(a), diffraction spots are strongly twisted, indicating that the crystalline periodicity has been severely disordered. The diffraction spots are oriented along three different directions, indicating that at least three crystal grains exist within the selected area. In contrast, the diffraction spots in Figure 3(b) are relatively regular with less deformation.

4. DISCUSSION

It has been reported that SiC undergoes phase transformation from the zinc-blende structure to the rocksalt structure in high-pressure (∼105 GPa) diamond-anvil cell tests.[10–14] Amorphization of SiC has also been demonstrated in micro cutting[15] and molecular dynamics (MD) simulations of nanoindentation.[16] In the present study, we did

not find amorphization of SiC, but detected its microstructural change to a poly crystalline phase. This structural change might be caused by two reasons: one is dislocation movement of under a high shear stress, and the other is phase transition under a high pressure. As the dislocation mobility of the zinc-blende SiC is very poor at room temperature, between the aforementioned two reasons the latter should be predominant. That is to say, in the region directly beneath the indenter tip (region A in Fig. 2(a)) where an extremely high pressure (~105 GPa) exists, SiC transforms from the zinc-blende structure to the rocksalt structure during loading. Dislocations are easier to move in the rocksalt structure, thus plastic deformation occurs. Then in unloading, a reverse transition from the rocksalt structure to the zinc-blende structure takes place, leaving a poly crystalline structure with intensive dislocations. It is presumed that this phase transformation only takes place around the indenter tip where the pressure is extremely high; in the surrounding region (region B in Fig. 2(a)) where the pressure is lower, phase transformation does not occur and elastic strain is dominant. To further clarify this issue, FEM analysis of the stress field in the nanoindentation tests is necessary.

5. CONCLUSIONS

Nanoindentation tests were performed on single crystalline silicon carbide (SiC) using a sharp Berkovich nanoindenter. The resulting indents were investigated by using a high resolution transmission electron microscope and the selected area electron diffraction technique. We found that the depth of indentation-induced subsurface damage is far larger than the indentation depth. Directly under the indenter tip, SiC changed into a poly-crystalline structure with a grain size of ten nanometer level. Micro cracks and basal plane dislocations together with possible cross slips were also found around the indent while no amorphous phase was confirmed. The results from this study strongly demonstrated that the subsurface damage mechanism of SiC is distinctly different from that of single crystalline silicon. These findings are important for renovating the manufacturing processes for high-quality SiC wafers.

References and Notes

1. T. Kimoto, *Technical Report of IEICE, Electron Devices* 104, 73 **(2004)**.
2. J. Yan, T. Asami, H. Harada, and T. Kuriyagawa, *Prec. Eng.* 33, 378 **(2009)**.
3. J. Yan, H. Takahashi, J. Tamaki, X. Gai, H. Harada, and J. Patten, *Appl. Phys. Lett.* 86, 1 **(2005)**.
4. J. Yan, H. Takahashi, J. Tamaki, X. Gai, and T. Kuriyagawa, *Appl. Phys. Lett.* 87, 1 **(2005)**.
5. J. Lankford and D. L. Davidson, *J. Mater. Sci.* 14, 1669 **(1979)**.
6. H. Kishimoto, K. H. Park, S. Kondo, K. Ozawa, and A. Kohyama, *J. Electr. Micro.* 53, 515 **(2004)**.
7. J. J. Huening Walter, M. Liang, X. B. Chen, J. Jang, L. Bergman, J. A. Patten, G. M. Pharr, and R. J. Nemanich, *Proc. Mater. Res. Soc. Symp.* 843 **(2005)**.
8. J. Yan, H. Takahashi, X. Gai, H. Harada, J. Tamaki, and T. Kuriyagawa, *Mater. Sci. Eng. A* 423, 19 **(2006)**.
9. K. Maeda, *J. Ceram. Assoc. Jap.* (in Japanese) 94, 784 **(1986)**.
10. M. Yoshida, A. Onodera, M. Ueno, K. Takemura, and O. Shimomura, *Phys. Rev. B* 48, 10587 **(1993)**.
11. M. S. Miao and W. R. L. Lambrecht, *Phys. Rev. B* 68, 092103 **(2003)**.
12. M. Durandurdu, *J. Phys.: Condens. Matter* 16, 4411 **(2004)**.
13. S. Eker and M. Durandurdu, *EPL* 84, 26003 **(2008)**.
14. Y. P. Lu, D. W. He, J. Zhu, and X. D. Yang, *Physica B* 403, 3543 **(2008)**.
15. J. A. Patten, W. Gao, and K. Yasuto, *Trans. ASME, J. Manuf. Sci. Eng.* 127–3, 522 **(2005)**.
16. I. Szlufarska, R. K. Kalia, A. Nakano, and P. Vashishta, *Appl. Phys. Lett.* 85, 378 **(2004)**.

Received: 4 September 2009. Accepted: 30 October 2009.